Paper:

Three-Fingered Gripper with Flexure Hinges Actuated by Shape Memory Alloy Wires

Daniela Maffiodo† and Terenziano Raparelli

Department of Mechanical and Aerospace Engineering, Politecnico di Torino
Corso Duca degli Abruzzi 24, Torino 10129, Italy
†Corresponding author, E-mail: daniela.maffiodo@polito.it
[Received August 16, 2016; accepted November 16, 2016]

A three-fingered gripper with flexure hinges actuated by shape memory alloy (SMA) wires was designed and prototyped. The aim of the work was the manipulation of small, almost cylindrical objects, e.g. test tubes, by a device having small overall dimensions. A parametric study of four different, but similar, fingers was conducted with the aim of obtaining a solution with a good amplification ratio and a gripping force almost constant during closure. The use of flexure hinges simplifies the design, but limits the finger range of motion. Moreover, it was possible to find a configuration with sufficient work space. Once the finger geometry was defined, the whole hand was then designed with the aim of producing a compact hand contained in a cylindrical volume (ϕ 65×h 65 mm), and the first prototype was built. Preliminary tests demonstrated its good dimensioning and the success of some technological solutions. The experimental transmission ratio was almost the same as the theoretical one. Some drawbacks have been highlighted, such as a reduced range of motion and incomplete backstroke; future studies will deal with them.

Keywords: shape memory alloy, gripper, flexure hinges

1. Introduction

In the last decades, research in the field of robotics has focused on non-conventional actuation, and one interesting possibility has been the use of shape memory alloy (SMA) actuators. These smart materials are widely used in industrial and robotic applications, representing a valid alternative to conventional actuators, especially when the reduced dimensions of the device highlight the SMA high power/weight ratio and there is no high frequency demand [1–2].

Robotic systems based on these innovative materials stand out because of their small dimensions, light weight, and simplicity, but to these characteristics one can add also the silent operation, the lack of contaminant production or use, and regular functioning, even in presence of electromagnetic disturbance.

The earliest examples of robotic hands actuated by SMA actuators were the four-fingered Hitachi hand (1984), which was designed for use in maintenance work, hostile environments, medical micro-manipulators, and undersea operations [3], a five-fingered biomechanic robot hand for flexible manipulation utilizing four Flexinol NiTi wires per finger [4], and a fingerspelling hand developed by Oaktree Automation, a hand that had 108 SMA wires acting in parallel, providing flexion and extension as well as abduction and adduction [5]. More recently, SMA finger and hand prototypes emulating human skeletal structures were proposed by De Laurentiis et al., Price et al., and Loh et al. [6–8]. Dulibal et al. [9] developed a robot with the special purpose of demining.

Bundoo et al. proposed an interesting solution for a prosthetic and wearable robotic hand based on the integration of compliant tendon cables and one-way SMA wires in an agonist-antagonist artificial muscle pair configuration to accomplish the different motions required of the finger joints [10]. Recently, various researchers have been working on these kinds of devices. One example is the multi-fingered prosthetic hand developed by Lee et al. [11], in which some SMA muscles were developed in order to increase its output force. Andrianesis et al. [12] designed a prosthetic hand with a new SMA-based actuation system, complete with closed-loop control.

The reduced dimensions of these devices make their design difficult. The use of flexure hinges leads to the reduction of the number of small parts in the device, helping the management of these difficulties. Moreover, flexure hinges have other advantages: they don't release wear particles and they don't add slip friction to the losses of the system. The angular range of motion of the flexure hinges can be low, but an adequate design of the system will allow for adequate finger displacement [13–16].

Some researchers have included flexure hinges in robotic systems. One interesting example is the Goldfard flexure-based gripper designed for manipulation tasks and actuated by a piezoelectric ceramic stack actuator [17]. Remarkable examples of robotic grippers with flexure hinges and actuated with SMA springs or ribbons are the Mertmann micro-miniature grippers [18].

Other examples of grippers actuated with SMA wires are the auto-adaptative gripper prototype designed by Manuello et al. with both parallel and angular finger motion [19] and a silicon microgripper for micromanipula-

Table 1. Finger configurations and relative displacement amplification ratio.

P0	P2
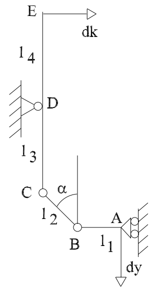 $\dfrac{dk}{dy}=\dfrac{l_4}{l_3}\cot\alpha$	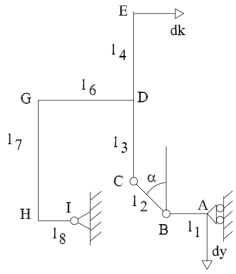 $\dfrac{dk}{dy}=\dfrac{\cos\alpha\cdot\sqrt{(l_6-l_8)^2+(l_4-l_4)^2}}{(l_6-l_8)\cos\alpha+(l_7-l_3)\sin\alpha}$
P1	**P3**
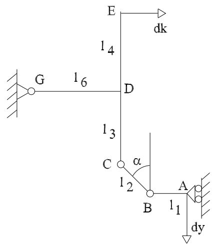 $\dfrac{dk}{dy}=\dfrac{\cos\alpha\cdot\sqrt{l_6^2+l_4^2}}{l_6\cos\alpha-l_6\sin\alpha}$	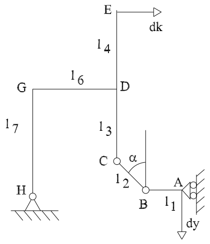 $\dfrac{dk}{dy}=\dfrac{\sqrt{l_6^2+(l_7+l_4)^2}}{l_6}\left(\dfrac{l_6\cot\alpha}{l_6\cot\alpha-l_7+l_3}\right)$

tion, designed by Raparelli et al. [20].

2. Parametric Analysis

The gripper has a cylindrical shape with three fingers in a polar array configuration, each finger placed 120° from the others. To choose the finger shape, different solutions were studied through kinematical analysis and compared. The displacement amplification ratios and the grasping force as a function of different geometrical quantities were graphed for four different fingers.

One specification for the design of this device was for it to have the possibility of assembling the actuation part of the device inside the arm body in order to protect it from collisions and dirt, but without hindering its motion. For this reason, the choice of the four configurations under study was made with the criterion of having the activation direction parallel to the principal lever in order to limit the radial dimensions of the device since it would be assembled inside the end of a robotic arm.

Table 1 shows the four finger configurations and the analytical formula for their displacement amplification ratio, defined as the ratio between the displacement *dk* of the finger end E and the displacement *dy,* imposed by the SMA actuator in A.

We chose to study the possibility of using flexure hinges because this would ensure a lightweight and simple device, but this implied that it was necessary to evaluate the maximum admissible rotation during the operation so as to prevent material yield. Moreover, the elastic torque generated was evaluated in order to consider its contribution to the bias force of the SMA wires. A bias spring was then added to the design, with the aim of pre-tensioning the SMA wires and of cooperating with the flexure hinges in the opening operation. The velocity ratio as a function of characteristic angles was studied for the chosen different solutions. This vectorial analysis was performed in order to obtain more information on the closing/opening motion, in particular to determine the senses of rotation for each hinge of the studied solutions and the critical conditions. These senses of rotation would be useful to define whether or not the use of a flexure hinge was allowable. The virtual work principle can be applied to verify the design of the device, taking into account the presence of flexure or traditional hinges and of bias springs. It is then possible to graph the force amplification ratio P/F, defined as the gripping force P at the finger end divided by the actuator force F, as a function of the geometrical quantities of the device, the variation of the angle α being particularly crucial, or as a function of the displacement amplification ratio dk/dy.

A parametric analysis was than carried out evaluating the displacement and force amplification ratio as a function of different geometrical parameters, in particular angle α and length l_1 to l_7 (see **Table 1**). Significant vari-

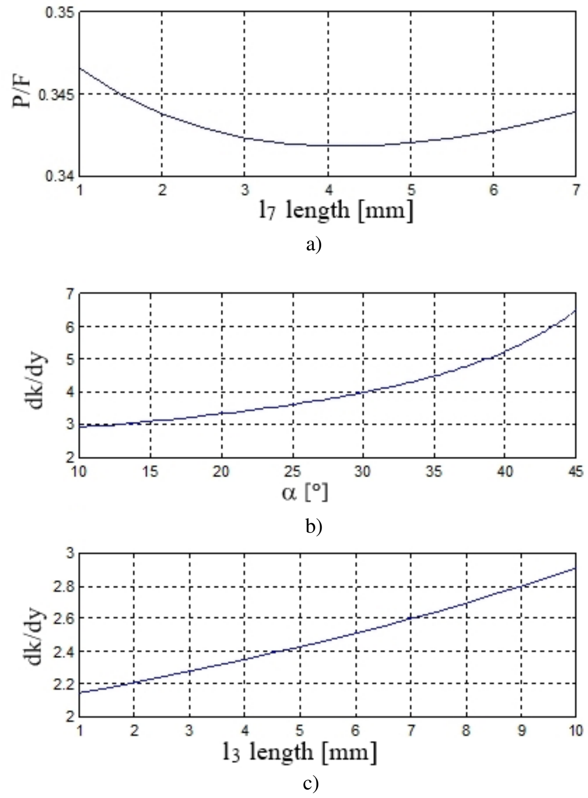

Fig. 1. Example of analysis for one P3 configuration: a) force amplification ratio P/F vs. l_7 length, $\alpha = 10°$, $l_3 = 10$ mm, $l_4 = 5$ mm, $l_6 = 5$ mm; b) displacement amplification ratio dk/dy vs. angle α, $l_3 = 10$ mm, $l_4 = 5$ mm, $l_6 = 5$ mm, $l_7 = 7$ mm; and c) displacement amplification ratio dk/dy vs. l_3 length, $\alpha = 10°$, $l_4 = 5$ mm, $l_6 = 5$ mm, and $l_7 = 7$ mm.

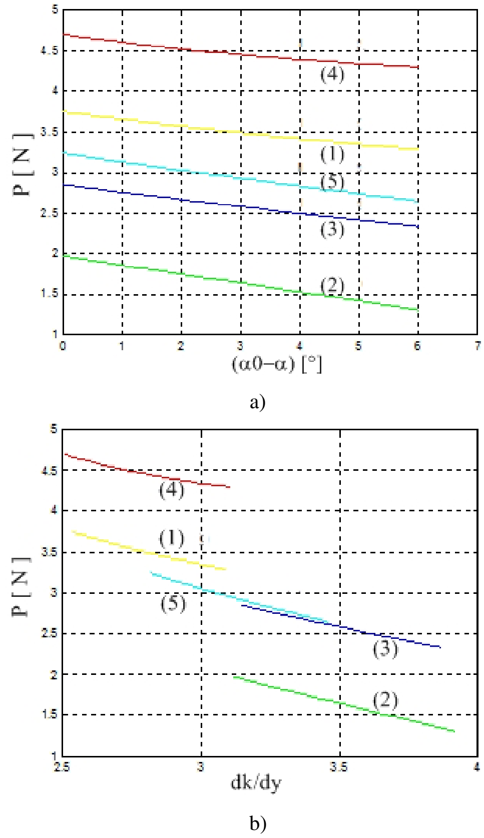

Fig. 2. Comparison between different P2 configurations a) gripping force P vs. angle variation $d\alpha$, b) gripping force P vs. displacement amplification ratio dk/dy; value of invariable quantities: $\alpha_0 = 66°$, $d\alpha = 6°$, $l_1 = 5$ mm, $l_2 = 6$ mm; value of parameters for curve (1): $l_3 = 9$ mm, $l_4 = 18$ mm, $l_6 = 11$ mm, $l_7 = 12$ mm, $l_8 = 7$ mm; value of parameters for curve (2): $l_3 = 10$ mm, $l_4 = 18$ mm, $l_6 = 11$ mm, $l_7 = 12$ mm, $l_8 = 9$ mm; value of parameters for curve (3): $l_3 = 10$ mm, $l_4 = 18$ mm, $l_6 = 11$ mm, $l_7 = 13$ mm, $l_8 = 8$ mm; value of parameters for curve (4): $l_3 = 6$ mm, $l_4 = 18$ mm, $l_6 = 11$ mm, $l_7 = 12$ mm, $l_8 = 9$ mm; value of parameters for curve (5): $l_3 = 8$ mm, $l_4 = 17$ mm, $l_6 = 12$ mm, $l_7 = 12$ mm, $l_8 = 9$ mm.

ations in trends are highlighted: slope inversions, asymptotes, etc.

As an example, **Fig. 1** presents three graphs for solution P3 with some parameters assigned (see caption under **Fig. 1**) and only one changing in each: in a) length l_7, in b) angle α, and in c) length l_3. **Fig. 2** shows the comparison of different solutions for the P2 solution. The caption under **Fig. 1** provides details.

An iterative method is used to reach one "good" solution, with the idea that good operation of the device is obtained when the amplification ratios and the grasping force have limited variation during the closing/opening of the hand. Moreover, some other critical situations were studied, such as the maximum rotation for the most loaded hinges.

Even though this analysis has limitations, it was very wide (more than 200 graphs were studied) so that a good result could be obtained.

At the end of this first analysis, the P3 solution was chosen as it worked best in terms of our specifications. With a 30×30 mm limit fixed for the finger dimensions, our following step was to perform a second analysis to increase the amplification ratio without reducing the finger end force too much while having a force trend as independent as possible from the amplification ratio.

We decided to make the fingers out of an AISI 420 stainless steel having $R_{s\min} = 1550$ N/mm^2 and $E = 2.1 \cdot 10^5$ MPa. The metal sheet thickness was 0.5 mm, and the width of the "bars" was 5 mm. The width of the reduced section was 2 mm; the hinge radius was 2 mm. Calculations on the flexure hinges were done following a traditional simplified method [10].

Since one finger weighed about 10^{-2} N, applying this weight to its center of mass, in the chosen configuration, would cause a moment on the virtual hinge of about $1 \cdot 10^{-4}$ Nm. Applying the formula from [10] for the rotation due to this moment, one could obtain a theoretical rotation of less than 0.08° due to the weight. This was considered negligible.

Moreover, for each configuration, the rotations of the flexure hinges during finger movement were studied as a function of the supposed displacement in A (see **Table 1**)

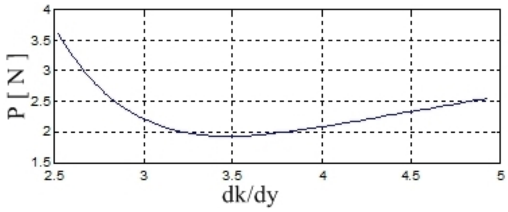

Fig. 3. Gripping force P as a function of the displacement amplification ratio dk/dy.

Fig. 4. Laser cut finger.

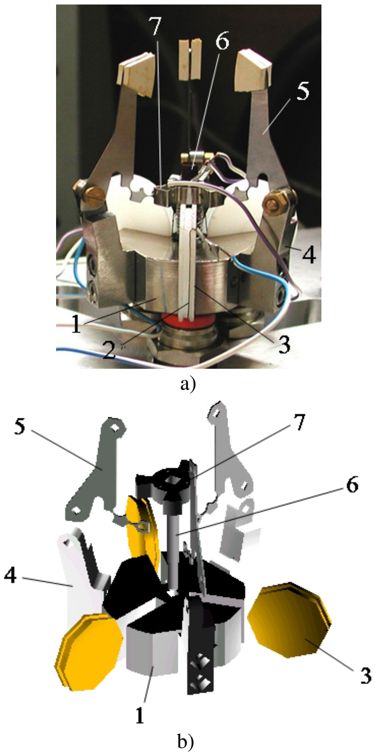

Fig. 5. a) exploded-view drawing of the robotic hand; b) picture: (1) metal base, (2) SMA wires, (3) plastic disks, (4) arms, (5) fingers, (6) central shaft, and (7) sliding star.

due to the shortening of the SMA wire fixed at that point.

Thanks to the material elasticity, a flexure hinge generated a rotational moment during the rotation caused by the SMA actuator. When the SMA wire was in its cooling phase, this moment could be used to create the bias force the SMA wire needed to return to the undeformed shape. Knowing the value of the bias force needed by the wire, one could hypothesize the dimensioning and verify if the material would yield in the reduced section when subjected to bending stress. Iterative calculations would allow one to find the proper dimensioning, compatible with the correct operation of the device.

At the end of this long process, we compromised by considering a traditional hinge at point A (see **Table 1**) and by adding a bias spring.

The final specifications of the device are as follows.

- $l_1 = 5$ mm, $l_2 = 6$ mm, $l_3 = 17$ mm, $l_4 = 13$ mm, $l_6 = 11$ mm, $l_7 = 18$ mm
- One finger overall dimensions $b \times h = 21 \times 33$ mm
- Hinge A is traditional. Hinges B and C (see **Table 1**) are flexure hinges.
- One SMA wire length $l = 11.2$ mm
- Force exerted by one SMA wire $F = 9.12$ N
- Expected force on the finger end $P_{\max} = 3.62$ N, $P_{\min} = 1.93$ N (see **Fig. 3**)
- Displacement amplification ratio $dk/dy_{\max} = 4.93$, $dk/dy_{\min} = 2.52$ (see **Fig. 3**)

Figure 3 shows the final graph of the gripping force P as a function of the displacement amplification ratio dk/dy.

The fingers were manufactured with laser cutting. The final shape can be seen in **Fig. 4**.

The final shape of the complete, three-fingered robotic hand is shown in **Fig. 5**; a) is an exploded-view drawing and b) is a picture. The metal base (1) has three equidistant cut-outs. Three SMA wires (2) are wrapped on three plastic disks (3) positioned inside the cut-outs. Three arms (4) are fixed to the base. Three fingers (5) are rigidly connected to the upper ends of the arms (4). A shaft (6) is mounted in the center of the base (1) to allow the vertical sliding of the sliding star (7). This sliding star is hinged to the A point of the fingers (see **Table 1**) and to one end of the three SMA wires. The opposite ends of the SMA wires are connected to the disks (3) by means of adequate cut-outs. When the wires are Joule heated, they shorten, causing the sliding star to slide down (7) and, as a consequence, the finger (horizontal translation of the finger upper end) to close.

3. Experimental Tests

Experimental tests were carried out to determine finger displacements and the experimental amplification ratio of the robot hand. A test bench, sketched in **Fig. 6**, was designed and assembled. The test was performed on the complete, three-fingered robot hand, but, to simplify the sketch, only one finger (1) is shown. The horizontal radial finger displacement was measured with an optical

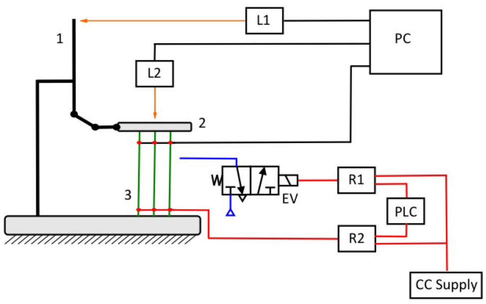

Fig. 6. Sketch of the experimental setup: (1) finger; (2) lifting star; (3) SMA wires, L1 and L2 laser sensors, R1 and R2 relay, EV pneumatic electrovalve.

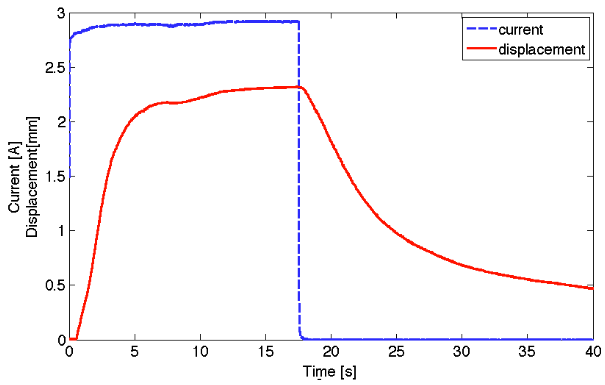

Fig. 7. Example of experiment: supply current (dashed blue line) and horizontal displacement of the finger end (continuous red line).

OMRON sensor (L1) pointed at one finger end. A second OMRON laser (L2) sensor was placed to measure the vertical displacement of the lifting star (2) (see **Fig. 5**).

The SMA actuators (3) (Flexinol Nitinol HT wire, diameter of 250 μm, phase change beyond 70°C) were supplied to generate the Joule heating and the subsequent shortening. Displacement and current data were then acquired by a PC. A flow of compressed air at an ambient temperature of about 25°C and pressure supply equal to 0.6 MPa (gauge), controlled by a pneumatic electrovalve EV (size 1/8”), cooled the SMA wires. The timing of the heating and cooling phase was managed by a PLC connected to two relays, R1 and R2.

Various tests were performed, both with compressed air cooling and without, for each finger. As an example, **Fig. 7** shows the results of one experimental test. The mean value of the finger end displacement is 2.5 mm. During the first 5 s, there is the maximum slope, then a less steep segment follows since the deactivation time is reached. The cooling phase time was different depending on whether the compressed air cooling had been activated or not. When the cooling system was switched on, the initial slope of the cooling was higher, but there was a decrease in the slope in the second cooling phase nonetheless, and the total cycle time, about 60 s, was similar with system on or off. Moreover, the movement of the three fingers was not exactly the same due to imperfections in the hand manufacturing, inaccurate SMA wire pre-tensioning, and the presence of friction. The total difference amounted to under 2%.

The hand shows an incomplete return to the undeformed conditions.

Grasping tests were performed, with the aim of verifying the ability to grasp a coin and plastic can, which are common objects with cylindrical symmetry. These tests had positive results; the grasping was precise and safe, as shown in **Fig. 8**.

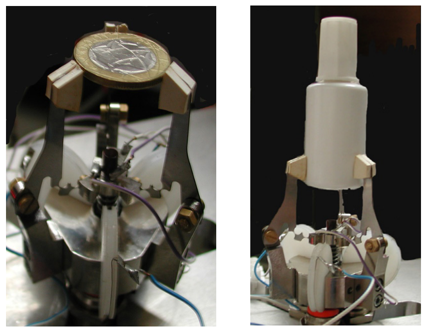

a) b)

Fig. 8. a) grasping a coin, b) grasping a plastic can.

To evaluate the hand’s ability to adapt to non-cylindrical objects, some grasping tests with objects having uneven shapes were performed. The tests showed that the hand had some ability to adapt, though the device was not conceived with this aim. Some anomalous finger rotations were noticed.

4. Conclusion

A lightweight and compact three-fingered robotic hand actuated by SMA wires has been produced. The fingers measure 21×33×0.5 mm, and the hand measures ϕ 65×h 65 mm overall. Actuation is performed by three SMA wires measuring 250 μm in diameter and 11.2 mm in length. The fingers have flexure hinges to simplify the device. The angular rotation of these hinges is limited to 2.5° out of a maximum of 3°.

The experimental amplification ratio is 2.2 versus a theoretical value of 2.8, but the mean displacement is less than a half of the expected value.

This is probably due to various factors. One is the presence of micro-sliding between plastic disks and SMA wires, but the main problem is probably the locking system for the wires. It is devoted to the anchoring and the supply of the SMA actuators, which not only causes reduced pre-tensioning of the wires but sometimes also sliding of the wire. This causes a reduction in the input displacement, which causes, as a normal consequence, a reduction in the output displacement.

Gripping tests showed good operation, and the grasping of cylindrical objects was safe and easy. Some operations were also performed on non-cylindrical objects, even though the device was not designed for such objects.

The hand's performance with non-cylindrical objects can be further investigated to measure the maximum admissible values of objects to be grasped eccentrically.

Future work to be done includes the use of the SMA wires' change in resistance as a sensor to develop a closed loop control of the robotic hand. The authors have already investigated this with a simple, straight SMA wire actuator [21] and wish to apply this idea to this gripper. Moreover, friction losses have to be reduced, and problems involving incomplete backstrokes must be solved on a new prototype that must have an improved locking system for the wires. Replacing the flexure hinges with traditional ones and increasing the lengths of the SMA wires can lead to an increase in the displacement of the finger ends, but an increase in the overall dimensions of the device could prove to be a drawback.

References:

[1] S. Hirose, K. Ikuta, and Y. Umetani, "A New Design Method of Servo-actuators Based on the Shape Memory Effect," in A. Morecki, G. Bianchi & K.Kedzior (Eds), Theory and Practice of Robots and Manipulators, MIT Press, Cambridge, MA, pp. 339-349, 1985.

[2] J. Sakurai and S. Hata, "Characteristics of Ti-Ni-Zr Thin Film Metallic Glasses/Thin Film Shape Memory Alloys for Micro Actuators with Three-Dimensional Structures," Int. J. of Automation Technology, Vol.9, No.6, pp. 662-667, 2015. (doi: 10.20965/ijat.2015.p06622)

[3] M. E. Rosheim, "Robot Evolution: The Development of Anthrobotics," John Wiley & Sons Inc., New York, 1994.

[4] I. Mihalcz, E. I. Zudor, V. Csibi, and P. Baranyi, "A biomechanic robot hand using SMA," Tenth World Con. on Theory of Mach. and Mechanisms, Oulu, Finland, pp. 1835-1840, June 1999.

[5] R. G. Gilbertson, "Muscle Wires Project Book," Third Ed., Mondotronics, Inc., California, 1994.

[6] K. De Laurentis and C. Mavroidis, "Mechanical Design of a Shape Memory Alloy Actuated Prosthetic Hand," Technology and Health Care, Vol.10, No.2, pp. 91-106, 2002.

[7] A. D. Price, A. Jnifene, and H. E. Naguib, "Design and control of a shape memory alloy based dexterous robot hand," Smart Mater. Struct., Vol.16, pp. 1401-1414, 2007.

[8] C. S. Loh, H. Yokoi, and T. Arai, "New Shape Memory Alloy Actuator: Design and Application in the Prosthetic Hand," Proc. of the 2005 IEEE Engineering in Medicine and Biology, 27th Annual Conf., pp. 1-4, 2005.

[9] S. Dilibal, R. M. Tabanli, and A. Dikicioglu, "Development of shape memory actuated ITU Robot Hand and its mine clearance compatibility," J. of Materials Processing Technology, Vol.155, pp. 1390-1394, 2004.

[10] V. Bundhoo, E. Haslam, B. Birch, and E. J. Park, "A shape memory alloy-based tendon-driven actuation system for biomimetic artificial fingers, part I: design and evaluation," Robotica, Vol.27, pp. 131-146, 2009. (doi: 10.1017/S026357470800458X)

[11] J. H. Lee, S. Okamoto, and S. Matsubara, "Development of Multi-Fingered Prosthetic Hand Using Shape Memory Alloy Type Artificial Muscle," Computer Technology and Application, Vol.3, pp. 477-484, 2012.

[12] K. Andrianesis, Y. Koveos, G. Nikolakopoulos, and A. Tzes, "Experimental Study of a Shape Memory Alloy Actuation System for a Novel Prosthetic Hand," In: Corneliu Cismasiu. Shape Memory Alloys. Croatia, Ed. Sciyo, 2010. (ISBN: 978-953-307-106-0)

[13] A. Midha, T. W. Norton, and L. L. Howell, "On the Nomenclature, Classification and Abstractions of Compliant Mechanisms," ASME J. of Mechanical Design, Vol.116, No.1, pp. 270-279, 1994.

[14] J. Paros and L. Weisbord, "How to design flexure hinge," Mach. Des., Vol.37, pp. 151-156, 1965.

[15] J. K. Yong, T-F. Lu, and D. C. Handley, "Review of circular flexure hinge design equations and derivation of empirical formulations," Precision Engineering, Vol.32, pp. 63-70, 2008.

[16] Y. Tian, B. Shirinzadeha, D. Zhang, and Y. Zhong, "Three flexure hinges for compliant mechanism designs based on dimensionless graph analysis," Precision Engineering, Vol.34, pp. 92-100, 2010.

[17] M. Goldfarb and N. Celanovic, "A Flexure-Based Gripper for Small-Scale Manipulation," Robotica, Vol.17, No.2, pp. 181-188, 1999.

[18] M. Mertmann and E. Hornbogen, "Grippers for the Micro Assembly Containing Shape Memory Actuators and Sensors," J. Phys. IV France, Vol.7, pp. C5-621-C5-626, 1997.

[19] A. M. Bertetto and M. Ruggiu, "A Two Degree of Freedom Gripper Actuated by SMA with Flexure Hinges," J. of Robotic Systems, Vol.20, No.11, pp. 649-657, 2003.

[20] T. Raparelli, P. Beomonte Zobel, and F. Durante, "Mechanical design of a 3-dof parallel robot actuated by smart wires," Proc. of EUCOMES 2008 - The 2nd European Conf. on Mechanism Science, pp. 271-278, 2009.

[21] D. Maffiodo and T. Raparelli, "Resistance Feedback of a Shape Memory Alloy Wire," Advances in Intelligent Systems and Computing, Vol.371, pp. 97-104, 2016. (doi: 10.1007/978-3-319-21290-6_10)

Name:
Daniela Maffiodo

Affiliation:
Assistant Professor, Department of Mechanical and Aerospace Engineering (DIMEAS), Politecnico di Torino

Address:
Corso Duca degli Abruzzi 24, Torino 10129, Italy

Brief Biographical History:

1995- Master Degree in Mechanical Engineering
1999- Researcher in DIMEAS, Politecnico di Torino
2002- Assistant Professor in DIMEAS, Politecnico di Torino

Main Works:

• G. Belforte, F. Colombo, T. Raparelli, and D. Maffiodo, "Study of the press forming mechanism of a thermoforming machine," Proc. of the Institution of Mechanical Engineers Part C, J. of Mechanical Engineering Science, London: SAGE Publications Ltd. Lancaster, PA: Technomic Pub. Co., Vol.228, pp. 9, 2014. (ISSN: 0954-4062, doi: 10.1177/0954406213499284)

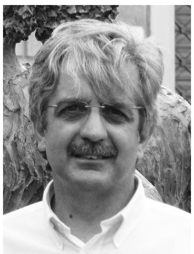

Name:
Terenziano Raparelli

Affiliation:
Professor, Department of Mechanical and Aerospace Engineering (DIMEAS), Politecnico di Torino

Address:
Corso Duca degli Abruzzi 24, Torino 10129, Italy

Brief Biographical History:

1983- Joined Politecnico di Torino
1992- Associate Professor at Politecnico di Torino
1994- Full Professor at University of L'Aquila
1999- Full Professor at Politecnico di Torino

Main Works:

• T. Raparelli, V. Viktorov, F. Colombo, and L. Lentini, "Aerostatic thrust bearings active compensation: Critical review," Precision Engineering, Vol.44, pp. 1-12, 2016. (ISSN: 0141-6359)

Membership in Academic Societies:

• Society of Tribologists and Lubrication Engineering (STLE)
• International Federation for the Promotion of Mechanism and Machine Science (IFToMM)
• Italian Association of Theoretical and Applied Mechanics (AIMETA)